LEGIBILITY NOTICE

A major purpose of the Technical Information Center is to provide the broadest dissemination possible of information contained in DOE's Research and Development Reports to business, industry, the academic community, and federal, state and local governments.

Although portions of this report are not reproducible, it is being made available in microfiche to facilitate the availability of those parts of the document which are legible.

3

Los Alamos National Laboratory is operated by the University of California for the United States Department of Energy under contract W-7405-ENG-36

LA-UR--89-2885

DE89 016616

TITLE PHONONS AND CHARGE-TRANSFER EXCITATIONS IN HTS SUPERCONDUCTORS

AUTHOR(S) A. R. Bishop, T-11

SUBMITTED TO Proceedings of "International School of Materials Science and Technology: Earlier and Recent Aspects of Superconductivity" Etore Majorana Cetre for Scientific Culture, Erice, Sicily, Italy; July 4-16, 1989. To appear in book of same title, eds. J. G. Bednorz and K. A. Mueller (Springer-Verlag, Heidelberg)

DISCLAIMER

Los Alamos National Laboratory
Los Alamos, New Mexico 87545

Phonons and Charge-Transfer Excitations in HTS Superconductors

A. R. Bishop

Theoretical Division
Los Alamos National Laboratory
Los Alamos, NM 87545 USA

Abstract. Some of the experimental and theoretical evidence implicating phonons and charge-transfer excitations in HTS superconductors is reviewed. It is suggested that superconductivity may be driven by a synergistic interplay of (anharmonic) phonons and electronic degrees of freedom (e.g. charge fluctuations, excitons).

I. Introduction

The wealth of experimental and theoretical studies of the new oxide superconductors begins to suggest more focused directions regarding mechanisms. While contributions from exotic and spin-based pairing mechanisms remain active possibilities, we believe that charge-transfer (CT) (excitonic) mechanisms synergistically assisted by electron-phonon coupling (and possibly accompanied by spin fluctuations) are indicated by a number of results and by the materials themselves. The high polarizability of O^{2-} and the familiar strong phonon modes and affinity for structural instabilities which characterize perovskite-like materials are ideal conditions to synergistically enhance low-lying metal-oxygen charge transfer channels. This is true of the simple layered 2-1-4 structures such as $La_{1-x}Sr_xCuO_4$ but is further augmented by the "sandwich" structures characterizing 1-2-3 $YBa_2Cu_3O_{7-\delta}$, Bi (4-3-3-4) and Tl (2-1-2-2), etc. In these latter cases we have proposed that the dynamic polarizability of the environment surrounding CuO_2 planes plays an important role in enhancing T_c.

Elsewhere [1] we have described how a large body of experimental information can be rationalized within such a theoretical scenario. Here we mention a few additional experimental facts which have become available more recently.

Raman scattering indicates certain strong phonon modes and the optical conductivity [2] has now converged on a picture of electrons scattering from "some" high frequency excitation in a phonon-like regime (500-700K): the implied high phonon frequency and strong interaction are certainly natural if oxygen is centrally involved, consistent with our discussion in section 2. The mid-IR absorption observed in the frequency dependent conductivity for $YBa_2Cu_3O_{7-\delta}$ thin films has now been resolved into a series of absorptions, probably of electronic (e.g. charge transfer (excitonic)) origin [3]. In an untwinned single crystal of $EuBa_2Cu_3O_{7-\delta}$ a strong mid IR feature has been observed [4] to be both narrow, polarized in the chain direction, and changing its frequency with δ, all consistent [5] with our theory of low-lying excitons in the Cu-O chains (see section 2(i)).

Phonons are also implicated by inelastic neutron scattering (suggesting, e.g., "breathing" modes in CuO_2 planes [6]), by (small) phonon anomalies which track T_c [7], and by tunneling data, particularly for $BiCaSrCu_2O_y$ [8]. Elastic constant anomalies appear as precursors of superconductivity in single crystal 2-1-4 samples. Strong electron-phonon coupling is almost certainly the driving mechanism in $Ba_xK_{1-x}BiO_3$ [9]. Strongly anharmonic phonons [6] may be suggested by recent neutron and Raman scattering evidence for more phonon branches than expected on symmetry grounds, as well as by apparent

doping-dependent isotope effects. In the 1-2-3 and high temperature Bi and Tl sandwich structures, recent copper K-edge XAS data suggest [10] that the O(4) "bridging" oxygen is characterized by a double well anharmonicity which is very sensitive in the superconducting transition region. This is highly suggestive of a synergistic coupling between the axial phonon dynamics and electronic degrees of freedom involved in the superconductivity. Such a picture is further supported by the anomalous oscillator strengths of axial O(4) phonons modes in both IR [7] and Raman [11]. In section 2(ii) we interpret this enhancement in terms of a coupling between phonons and CT electronic modes -- which we have elsewhere (see section 2(i)) also suggested as driving the superconductivity. The scenario of strongly nonlinear (e.g., Jahn-Teller-, buckling-, tilting-, or breathing-mode) phonons, perhaps coupled to CT excitons or spin fluctuations, may also occur in the CuO_2 planes of the 2-1-4 materials, but data is incomplete so far [6], although evidence for anomalous Raman activity of specific plane modes is beginning to appear. The ubiquitous large linear resistivity temperature regime could also be ascribed to the presence of two dominant phonons/excitons: electron interactions with a low frequency mode ($\hbar\omega \lesssim k_B T_c$) could drive T_c, while scattering from high frequency modes ($\hbar\omega \gg k_B T_c$) would dominate resistivity.

Some recent tunneling [8] and photoemission [12] data have suggested strong coupling BCS-like behavior with $2\Delta(o)/k_B T_c \sim 7$. This is somewhat high for conventional strong coupling Eliashberg theory with linear phonons and Coulomb effects controlled by μ^*. However a synergistic coupling of e.g. nonlinear phonons, or phonons and CT excitons (as suggested above) has yet to be investigated systematically. Again, strong Coulomb interactions, strong coupling between phonons and superconductivity, or anistropic pairing, will take us beyond the conventional Eliashberg framework. We will reemphasize these issues in section 3.

Our primary intention here will be to summarize some of the model Hamiltonians being employed to address aspects of the scenario outlined above.

2. Models Hamiltonians and Charge Transfer

Deciding on an appropriate microscopic model hamiltonian to describe the complex structures of the new materials is not straightforward and not a settled issue: 1-band or multiband; π- or σ- or other orbitals?; 2-dimensional or (anistropic) 3-dimensional? Interpreting experimental probes lags the quality of the measurements themselves in some cases, and sample quality continues to be a limiting issue for characterizing intrinsic properties. Interpreting photoemission so as to extract model parameters is still controversial, although band structure and various degrees of ab initio quantum chemistry are now converging with respect to parameter assignments for Hubbard models. However, since we believe that Hubbard models will eventually have to be seriously extended in these materials (via anharmonic electron-phonon coupling [13], Hubbard V,W [14,15], multiple-bands [15], etc.), it remains premature to attempt to fix model parameter values. We therefore prefer to explore parameter space widely in simple models and allow experiment to guide the most important augmentation of those models. With this philosophy in mind, we describe here (i) a U-V Hubbard model; (ii) a local charge-transfer-phonon cluster model; (iii) a "+ve U" model of BCS superconductivity; and (iv) a 1-dimensional analog system. Each model allows us to address different aspects of the puzzle.

We first consider a single CuO_2 plane. One of the simplest Hamiltonian that takes into account both Cu and O sites can be written:

$$H = \varepsilon_d \sum_i d_i^\dagger d_i + \varepsilon_p \sum_j p_j^\dagger p_j - \sum_{(i,j)} t_{i,j} d_i^\dagger p_j + h.c$$

$$+ U_d \sum_i n_{d\uparrow i} n_{d\downarrow i} + U_p \sum_j n_{p\uparrow j} n_{p\downarrow j} + V \sum_{(i,j)} n_{d,i} n_{p,j} \ . \qquad (1)$$

where $t_{i,j}$ is the hopping matrix element between Cu $d_{x^2-y^2}$ and O $p_{x,y}$ orbitals, ε_d and ε_p are respective local energy levels, $U_d(U_p)$ is the onsite Coulomb repulsion and V is the nearest-neighbor Coulomb repulsion between Cu and O sites. Since *both* spin and charge fluctuations can be soft, Hamiltonian (1) differs qualitatively from the Hubbard Hamiltonian, where charge fluctuations are suppressed. If we ignore U_d, U_p and V the resulting band structure consists of bonding (B) and antibonding (AB) Cu-O bands along with a flat nonbonding (NB) oxygen band [16,17]. At stoichiometry in La_2CuO_4 and $YBa_2Cu_3O_6$ the 2D AB band is $\frac{1}{2}$-filled and these materials should be metals. On the contrary, experimentally both exhibit antiferromagnetism [18,19], indicating the importance of correlations. To understand the effect of correlations in (1) we will first use weak coupling theory which enables explicit evaluation of relevant quantities. We find that the physics in the superconducting regime is dominated by low lying charge transfer excitations. Since oxide superconductors appear to be more in the intermediate coupling regime, our result should be interpreted in a qualitative sense. However, quantum chemistry calculations for finite clusters (below) also demonstrate the importance of charge transfer excitations. We therefore expect that overall features of our theory persist in the intermediate coupling regime, and this has indeed been supported by a variety of calculations in the strong coupling regime using, e.g. slaved-boson analytic techniques [20], exact numerical diagonalizations or quantum Monte Carlo [21].

Consider the case when the AB band in the CuO_2 plane is $\frac{1}{2}$-filled. After projecting the Hamiltonian (1) onto the AB band we obtain the following effective Hamiltonian:

$$H_{AB}^{eff} = \sum_{\vec{k},\sigma} \xi_{\vec{k}} c_{\vec{k},\sigma}^\dagger c_{\vec{k},\sigma} +$$

$$+ \sum_{\vec{k},\vec{k}',\vec{q}} \sum_{\sigma,\sigma'} [\tilde{U} + 2\tilde{V}\cos(q_x a) X_{\vec{k}+\vec{q}} X_{\vec{k}} + 2\tilde{V}\cos(q_y a) Y_{\vec{k}+\vec{q}} Y_{\vec{k}}] c_{\vec{k}-\vec{q},\sigma'}^\dagger c_{\vec{k}+\vec{q},\sigma}^\dagger c_{\vec{k},\sigma} c_{\vec{k}',\sigma'} \ , \qquad (2)$$

where a is the Cu-O separation, $\xi_{\vec{k}} = \frac{1}{2}(\varepsilon_d + \varepsilon_p) - \mu + \frac{1}{2}[(\varepsilon_d - \varepsilon_p)^2 + 16t^2(\sin^2 k_x a + \sin^2 k_y a)^2]^{\frac{1}{2}}$, $\tilde{U} \equiv U_d \cos^4\theta + U_p \sin^4\theta$, $\tilde{V} \equiv V \cos^2\theta \sin^2\theta$, with $\cos^2\theta = \frac{1}{2} + \frac{1}{2}[1 + \frac{16r^2}{(\varepsilon_d - \varepsilon_p)^2}]^{-\frac{1}{2}}$, r being the average of the Cu-O hybridization over the Fermi surface. $X_{\vec{k}}$ and $Y_{\vec{k}}$ are coherence factors.

In weak coupling, we can study collective modes of the system by considering the equation for the response function $\chi_{\sigma,\sigma'}(\vec{q},\omega)$ arising from the sum of ring and ladder diagrams:

$$\chi_{\sigma,\sigma'}(\vec{q},\omega) = \chi_0(\vec{q},\omega) + \delta_{\sigma,\sigma'}\chi_0(\vec{q},\omega) I(\vec{q}) Tr\,\chi(\vec{q},\omega) - \chi_0(\vec{q},\omega) J(\vec{q}) \chi_{\sigma,\sigma'}(\vec{q},\omega) \ . \qquad (3)$$

where $\chi_0(\vec{q},\omega)$ is the Lindhard function in the AB band and we have restricted our attention to the interband response. The direct interaction $I(\vec{q})$ and exchange interaction $J(\vec{q})$ follow from (2):

$$I(\vec{q}) = \tilde{U} + 2\tilde{V}\cos(q_x a)\alpha_x(\vec{q}) + 2\tilde{V}\cos(q_y a)\alpha_y(\vec{q}) \ , \tag{4}$$

$$J(\vec{q}) = \tilde{U} + 2\tilde{V}\sum_{i=1}^{2}(|\beta_x^i(\vec{q})|^2 + |\beta_y^i(\vec{q})|^2) \ . \tag{5}$$

In the above equation we have used the definitions:

$$\alpha_x(\vec{q}) \equiv \chi^{-1}(\vec{q}, \omega = 0)\sum_{\vec{k}} K_0(\vec{k}, \vec{q})\gamma_{\vec{k}+\vec{q}}\gamma_{\vec{k}} \ ,$$

$$\beta_x^i(\vec{q}) \equiv \chi^{-1}(\vec{q}, \omega = 0)\sum_{\vec{q}} K_0(\vec{k}, \vec{q})\gamma_{\vec{k}+\vec{q}}\gamma_x^i(\vec{k}) \ ,$$

where $\gamma_x^1 = \cos k_x a$, $\gamma_x^2 = \sin k_x a$. $K_0(\vec{k}, \vec{q})$ is defined by $\chi_0(\vec{q}, \omega = 0) \equiv \sum_{\vec{k}} K_0(\vec{k}, \vec{q})$. The definitions of quantities with subscript y are obvious.

At half-filling the Fermi surface has perfect nesting and there will be a tendency to open a gap on the Fermi surface. An instability can occur in both the charge and spin density channels and the resulting CDW and SDW will have periodicity determined by the nesting vectors $\vec{Q}_0 = (\frac{\pi}{2a}, \pm\frac{\pi}{2a})$. One can show by solving (3) that the relative stability of a CDW or SDW depends on the sign of $I(\vec{q})$: First note that $\chi_0(\vec{Q}_0, \omega = 0) \propto -\frac{1}{D}\ell n^2(\frac{\beta}{4})$, where $D \sim 2t$. From (3) follows $\ell n^2(\frac{D}{T_{SDW(CDW)}}) = \lambda_{SDW(CDW)}^{-1}$, where $\lambda_{SDW} \propto J(\vec{Q}_0) > 0$ and $\lambda_{CDW} \propto J(\vec{Q}_0) - 2I(\vec{Q}_0)$, $T_{SDW(CDW)}$ being the transition temperature of spin (charge) density wave. Obviously, for positive $I(\vec{Q}_0)$ $T_{SDW} > T_{CDW}$, while for negative $I(\vec{Q}_0)$ the situation is reversed. Since $I(\vec{Q}_0) = \tilde{U} > 0$ the ground state in weak coupling is SDW, *irrespective* of the relative size of $\tilde{U}$ and $\tilde{V}$. This SDW reflects the qualitative features of the observed antiferromagnetic state. Thus, the *intraband* particle-hole excitations arising in (1) account for the antiferromagnetism of these compounds.

However, away from half-filling, when holes are added to the system either by doping or by varying oxygen content, the situation may change qualitiatively. This can be appreciated by considering $\chi_0(\vec{q}, \omega = 0)$. As x holes are added to the AB band, the maximum of $\chi_0(\vec{q}, \omega = 0)$ moves from $\vec{Q}_0$ to some $\vec{Q}(x)$, such that $|\vec{Q}(x)| < |\vec{Q}_0|$ and $2\tilde{V}\alpha_x(\vec{Q}(x))\cos Q_x(x)a + 2\tilde{V}\alpha_y(\vec{Q}(x))\cos Q_y(x)a$ becomes progressively more negative. (Note that $\alpha_{x,y}(Q(x)) < 0$). The maximum occurs for $\vec{Q}(x) = (\pm Q, \pm Q)$ where $Q \simeq \frac{\pi}{2a} - \frac{\mu'}{t}$, for $\varepsilon \ll t$ and $\mu' \equiv 2t - \mu$. The relation between x and μ is $x \simeq (\frac{\mu'}{2t})\ell n(\frac{2t}{\mu'})$. For $\tilde{V}$ large enough it is possible to attain a situation where:

$$I(Q_{y(x)}) = \tilde{U}(x) + 2\tilde{V}(x)\alpha_x(\vec{Q}(x))\cos Q_x(x)a + 2\tilde{V}(x)\alpha_y(\vec{Q}(x))\cos Q_y(x)a < 0 \ , \tag{6}$$

for some concentration of holes $x > x_c$, x_c being defined by $I(\vec{Q}(x_c)) = 0$. This signals the preference for CDW formation. The real, static CDW deformation does not occur, however, since away from half-filling the nesting features are diminished. We then have *low-lying*, finite wavevector ($\vec{Q}(x)$), temperature independent, collective charge excitations in the CuO_2 plane, which will strongly influence the effective electron interactions. For some region of doping $0 < x_c \leq x \lesssim x_s < 1$, which can be calculated from (3), the

frequency of these short wavelength charge fluctuations $\omega_{CF}(\vec{Q}(x))$ will be lower than the corresponding spin fluctuation frequency $\omega_{SF}(\vec{Q}(x))$, and they can be utilized to build an attractive retarded interaction which can lead to superconductivity. Such a region will occur only for $\varepsilon \equiv \varepsilon_d - \varepsilon_p \lesssim t$ and for $V \gtrsim \frac{1}{4}U$. Explicit results for the frequencies of collective modes illustrating this crossover are given in [22]. The generic behavior is shown in Fig. 1(a). The upturn in ω_{CF} is caused by a decrease of $\bar{V}$ as one empties the AB band.

Note that our *intraband* charge excitation is distinct from the local charge transfer exciton proposed in [23], although the underlying theme, relying on the low energy cost for Cu $\leftrightarrow$ O charge transfer (see below), is similar. Softening of *interband* charge fluctuations is driven by V alone [22,23] but are importantly enhanced by local field effects [23].

We now discuss superconductivity. Following the Eliashberg formalism outlined in [24] we define the matrix element of the pairing interaction,

$$\lambda_{CF(SF)}(\vec{k},\vec{k}') = -2\alpha^2_{CF(SF)} \int_0^\infty d\omega \frac{F(\vec{k},\vec{k}';\omega)}{\omega} , \qquad (7)$$

where $\alpha_{CF(SF)}$ is the electron-charge fluctuation (spin fluctuation) vertex, and $F(\vec{k},\vec{k}';\omega)$ is given by $-\frac{1}{\pi}\mathrm{Im}\chi^{CF(SF)}(\vec{k},\vec{k}';\omega)$, where $\chi^{CF(SF)}(\vec{k},\vec{k}';\omega)$ is obtained from (3). In (7) $\vec{k}$ and $\vec{k}'$ are constrained to lie on the Fermi surface. We have used the solution of Eq. (3) to evaluate (7) in various orbital states as a function of model parameters. In Figure 1(b) we show the typical results for the ground state of the CuO_2 plane as a function of x. We have set $\varepsilon = 0$. SC I is a d-wave superconductivity, produced by low-lying spin fluctuations. In this region T_c is expected to be *low*, due to self-energy corrections and dynamic pair-breaking. For $x > x_c$, the superconductivity crosses over to the s-wave type (SC II), where charge fluctuations dominate and T_c may be higher since the above limitations are absent for an isotropic superconducting state. High T_c's are still problematical in pure C-T pairing because of competing trends of coupling constants and μ^*, however it is very important to note (see below) that *phonons* may enhance T_c in SC II phase (they basically have no effect in SC I). Since T_c calculations are notoriously unreliable one should interpret our results as representing qualitative trend produced by doping the AB band. Finally, for large doping, the AB-NB *interband* charge fluctuations can lead to a CDW phase, a charge disproportionated state with a "frozen-in" Cu $\leftrightarrow$ O charge transfer and lattice distortion. In the shaded regions there is a competition between different ground state symmetries and it is possible that the system is a metal at T = 0. This phase diagram is very suggestive of a similarity between high T_c oxides and the "old" Ba-Pb-Bi-O superconductor [25,26]. The newly discovered K-Ba-Bi-O superconductor increasingly clearly belongs to the same class.(9) This behavior is also in qualitative agreement with recent data on the 2-1-4 material which indicate that T_c saturates at 40K for x between 0.15 and 0.25 and then drops quickly to zero at $x \sim 0.30$ [27]; data on T_c in 1-2-3 materials as a function of hole density in the plane now appears to be similar [28].

Why is T_c much higher in 1-2-3 and the new Bi and Tl systems than in 2-1-4? We conjecture [1] that the dynamic polarizability of the environment of CuO_2 planes is crucial for elevating T_c. As an *illustration*, we consider $YBa_2Cu_3O_{6.9}$ specifically. Consider a single Cu-O chain along the y-axis. (We emphasize that chains are <u>not</u> crucial to our general concept.) We can use the same Hamiltonian (1) where now the relevant atomic orbitals are Cu $d_{y^2-z^2}$ and O p_y. In 1D there is perfect nesting at any band filling. The ensuing instability is driven by deformation of wavevector $Q_y = 2k_F^c$. Just as in the plane, as holes are added to the AB band, Q_y decreases from $\frac{\pi}{2a}$ ($\frac{1}{4}$-filled) to 0 (AB band empty), and $I(Q_y)$ can become negative, leading to strong charge fluctuations. The actual CDW

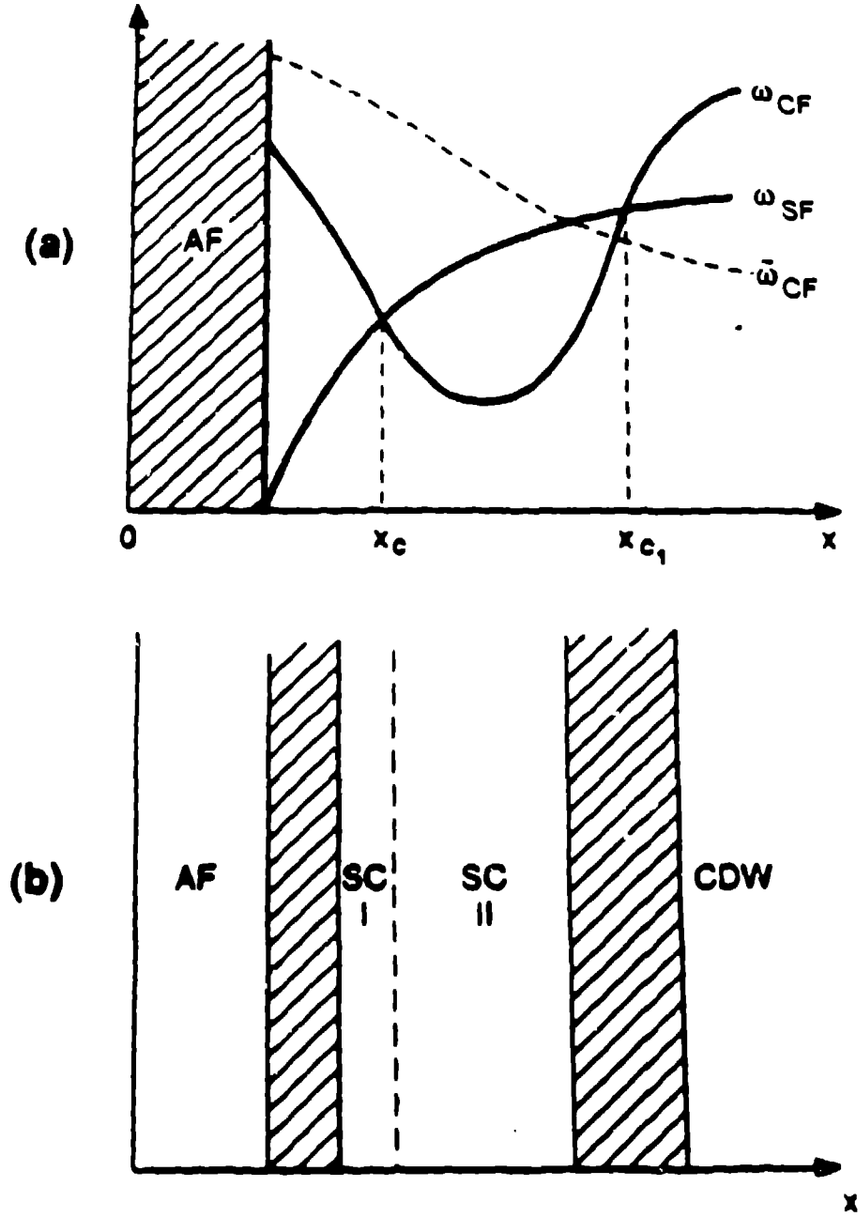

Figure 1. a) the generic x-dependence of ω_{SF} and ω_{CF} for CuO_2 plane. The region of $\omega_{CF} < \omega_{SF}$ occurs only for sufficiently large $\tilde{V}/\tilde{U}$ as explained in text. $\bar{\omega}_{CF}$ refers to the interband charge excitations which may lead to the CDW (charge disproportionation) distortion at high doping. b) The qualitative ground state phase diagram as a function of x. Different regions are discussed in text. A CDW phase is most likely for $\epsilon = 0$.

instability is prevented by hopping, $t_\perp$, between chains and planes, by quantum fluctuations, and by disorder. The reduced dimensionality, however, is likely to make chains more polarizable than planes. In this way we use the high polarizability of a 1D system at wavevector $2k_F^c$ to further enhance an intrinsic polarizability of the Cu-O bond (see below). The high polarizability of the chains will affect the electron-electron interactions on neighboring planes, via an effective chain-plane Coulomb coupling, W. This effective interaction for electrons on planes is given by $n_c|W|^2\mathrm{Tr}\chi^{chain}(q_y,\omega)$, where n_c is the linear density of chains. Note that, this interaction is the *same* for two electrons on adjacent CuO_2 planes or on a single plane.

In reality the situation in $YBa_2Cu_3O_{6.9}$ is more complicated. In addition to the linear Cu-O chain, there are bridging oxygens (O(4)), which control the plane-chain coupling, W. The presence of these oxygens induces additional transverse polarization of the chains, favoring intraplane pairing. This mode is a part of an *interband* response, not included in (3). Consider the cluster in Figure 2a. The upper and lower Cu have the coordination of the planes (Cu_p), while the central atom is a unit of the chain (Cu_c). The orbitals of particular interest are the $d_{x^2-y^2}$ orbitals on the Cu_p, the $d_{y^2-z^2}$ orbital on Cu_c, and the p_z oribtals on the bridging O(4) oxygens. Note that the bridging O p_z orbitals have the wrong symmetry to interact directly with $d_{x^2-y^2}$, but can interact with the $d_{y^2-z^2}$ orbital. These three atomic orbitals on the chain combine to give B, NB, and AB molecular orbitals. The NB orbital will develop into a narrow O p_π band along the chain axis involving O p_z orbitals, while the AB orbital develops into the Cu $d_{y^2-z^2}$ band considered above. Current *ab initio* quantum chemistry calculations [29] on the cluster in Figure 2 suggest that the interband charge transfer mode, in which an electron moves between the NB O p_π orbital and the AB Cu $d_{y^2-z^2}$ band, occurs at low energy, ω_t, of the order of a few 0.1 eV, and that the ground state of the Cu_3O_{12} cluster model for $YBa_2Cu_3O_{6.9}$ involves an "empty" Cu $d_{y^2-z^2}$ orbital and a pair of electrons in the O p_π NB orbital ($Cu^{3+}-O^{2-}$). The state in which the electron is excited from the NB orbital to $d_{y^2-z^2}$ ($Cu^{2+}-O^{1-}$) lies a few 0.1 eV above the ground state. Which of these two states has lower energy depends on the nature of the correlations included in the configuration interaction. The common denominator in all our calculations, however, is the presence of low-lying charge transfer excitations. By contrast, in cluster models of $YBa_2Cu_3O_{6.5}$ the lowest charge transfer excitations occur at energy $\sim$ several eV.

If the above clusters are ordered in chains, there will be strong plane-chain Coulomb coupling, since both the intraband and interband excitations lead to rearrangement of the charge distribution on the bridging oxygens. The strength of the pairing interaction should scale approximately as $\frac{1}{r_1^7}$, where r_1 is the Cu(2)-O(4) distance. With both types of charge transfer excitations included, the retarded attraction will be somewhat stronger with the electrons on the same plane. Nevertheless, the beauty of the $YBa_2Cu_3O_{6.9}$ sandwich structure is that the bridging oxygens can couple two distinct planes, and we might even expect that the system will still take advantage of interplane pairing, thereby defeating in large part the direct Coulomb repulsion. The most favorable situation for interplane pairing would occur in orthorhombic $YBa_2Cu_3O_{6.9}$ with highly ordered chains, where the longitudinal intraband exciton could be dominant. Estimates of T_c and gap function symmetry have been given in [1], including both longitudinal and transverse excitons, and intra- as well as inter-plane pairing. Alternative scenarios for the role of off-plane polarizations enhancing or driving in-plane superconductivity are outlined in section 3.

We emphasize that many related chain complexes (see section 3(iv)) have strong CDW (charge disproportionation) tendencies, which are further strengthened by coupling to the

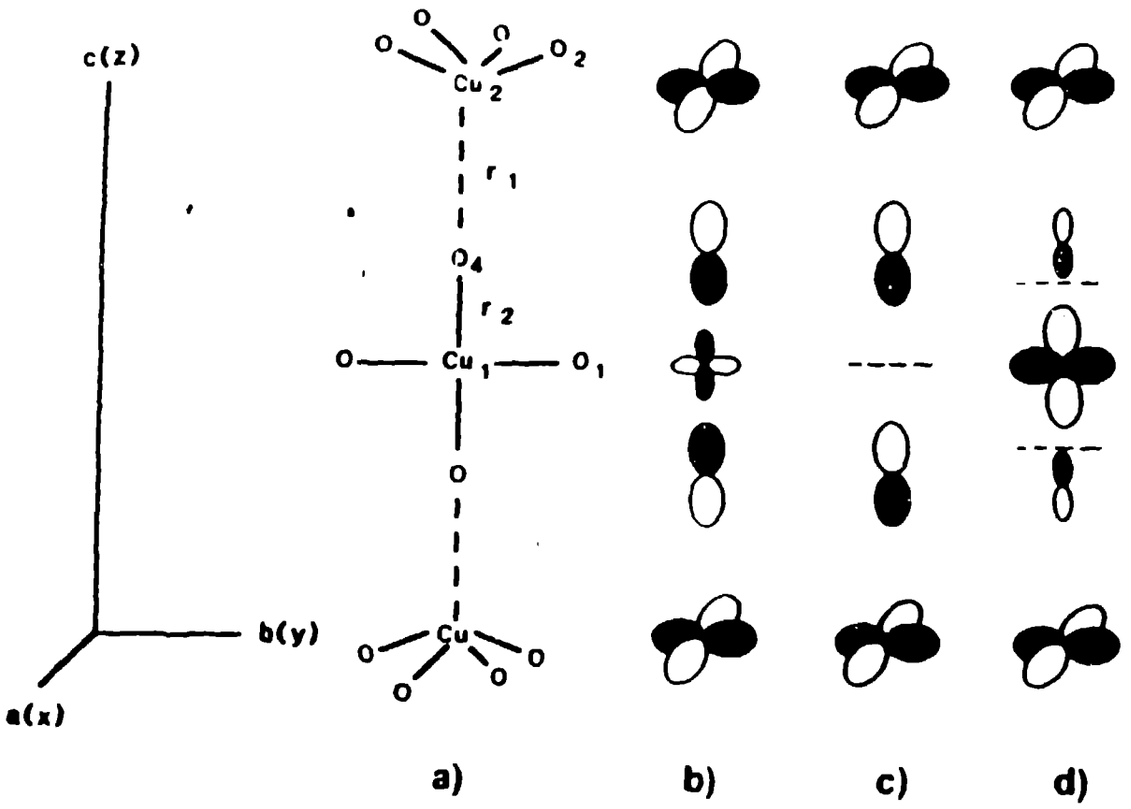

Figure 2. a) Cu_3O_{12} cluster model of the PCP-like structure. b), c) and d) denote the B, NB and AB combinations, respectively. The phase of an atomic orbital is denoted by shade. The Cu $d_{x^2-y^2}$ orbitals in the planes are pictured for the readers orientation: they do not interact with the O p_z orbitals.

lattice. Therefore, it is indeed plausible to expect that the physics of Cu-O chains in $YBa_2Cu_3O_{6.9}$, with electron-phonon interactions and out-of-chain (plane) O polarizations included, is dominated by their proximity to a CDW.

2(ii) Charge-transfer-phonon coupling:

Here we present a simple three level cluster model [30] which addresses the possibility that charge transfer fluctuations are responsible for the anomalously large intensity of the 155 cm^{-1} Ba mode observed by Cenzel et al. (7) The model also relates to the accompanying Raman signature and the c-axis anomaly observed by Cava et al., [31] and suggests that these features should be related to a change in the hole density in the plane.

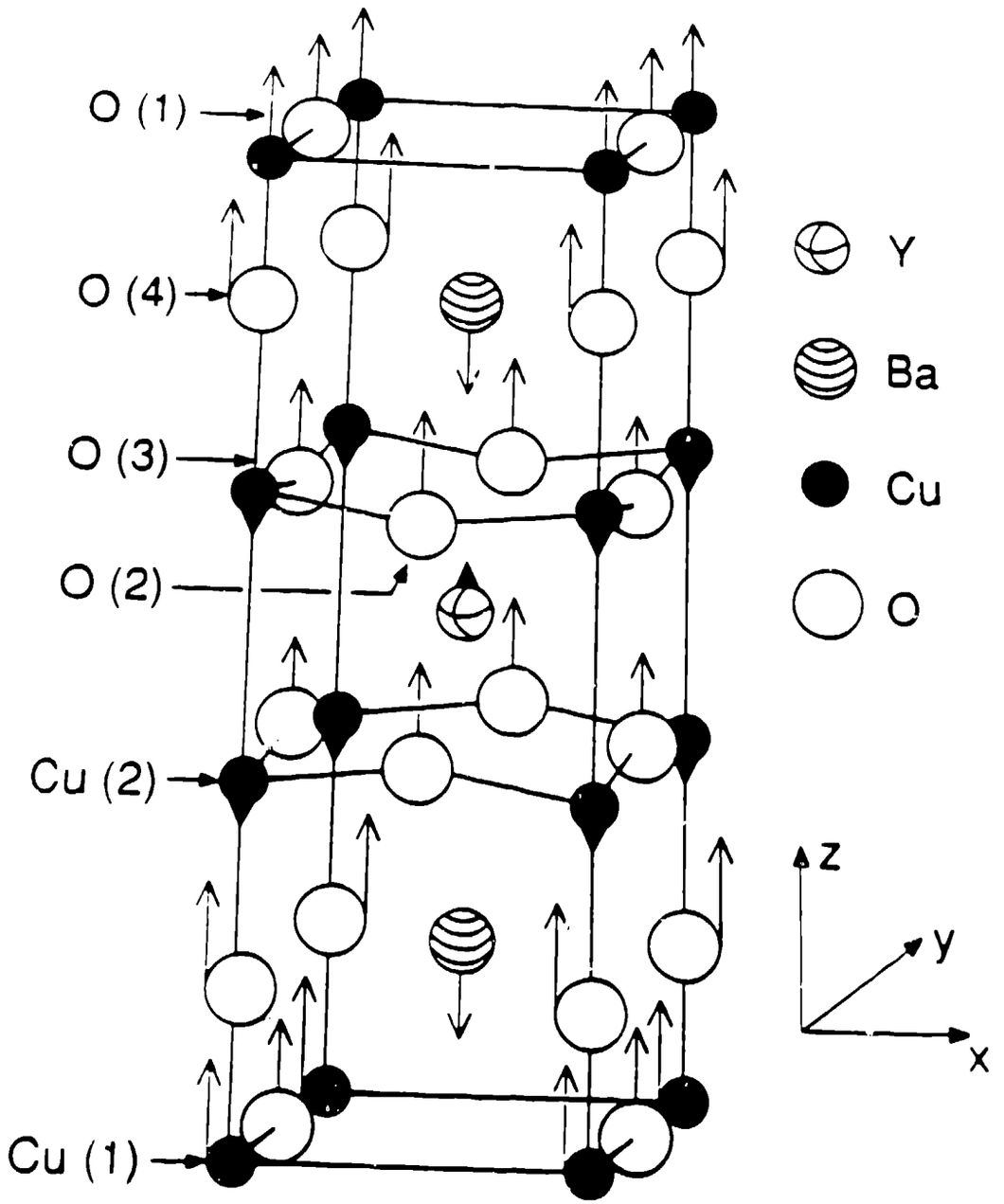

Figure 3. Unit cell of $YBa_2Cu_3O_7$ with the relative ionic displacements of the "Barium mode" at 153 cm^{-1}. (After ref. [7].)

Anomalously large oscillator strengths have been reported for the IR phonon mode observed in $YBa_2Cu_3O_{7-\delta}$ at 155 cm^{-1} for $\delta \sim 0$. This mode has been labeled as the "Barium" mode and it can be quite accurately described as a rigid motion of the $[CuO_3]$ cluster (chain+two $O4$) in one direction and Ba^{+2} ions in the opposite direction, (Fig. 3). The oscillatory strength of this mode was found to be ~15 times larger than the prediction of a pure latrice dynamics calculation.[7] This is of course consistent with our earlier discussion here of the importance of the c-axis activity.

We assume that the charge of a CuO_3 cluster in the $YBa_2Cu_3O_7$ system is -4. There are several reasons for such a thesis. If the charge of the cluster is equal to -3, then the charge of the conducting planes CuO_2 should be -2, which implies half filling of the conducting band, and the appearance of the antiferromagnetism. This is in contradiction with the observation of superconductivity in $YBa_2Cu_3O_7$. However, if the charge of the cluster is -4, or more realistically the average is between -3 and -4, then the charge of the planes is less than -2. The finite density of holes in the conducting band may then lead to superconductivity as in doped La_2CuO_4. In oxygen deficient samples, a part of the electrons from the oxygens lacking in the $CuO_{3-\delta}$ cluster is presumably transferred to the plane. This transfer will suppress the superconductivity, but will also result in a structural transformation along the c-axis, as has been indeed observed by Cava et al.[31] Additional experimental support for our assignment are the X-ray absorption measurements of Tranquada et al.[32] They have found that the "doping" (=reduction of oxygen content) increases the number of Cu^{+1} ions per unit cell from zero to 1 on account of the reduction in the number of Cu^{+2} ions; They have attributed Cu^{+1} ions to the chains ($Cu1$). We also note that Monien and Zawadowski [33] have recently given a complementy discussion of Fano-like Raman scattering enhancement by electronic degrees of freedom in a 2-band CT model and coupling to a specific (buckling) oxygen plane mode at $\simeq$ 330 cm^{-1}.

Assuming therefore that the total charge of the CuO_3 cluster is -4, we have only four formal charge states of the cluster with the charge configurations,

$O4^{-1}$	$O4^{-2}$	$O4^{-2}$	$O4^{-2}$
|	|	|	|
$Cu1^{+1} - O1^{-2}$	$Cu1^{+2} - O1^{-2}$	$Cu1^{+1} - O1^{-2}$	$Cu1^{+1} - O1^{-1}$
|	|	|	|
$O4^{-2}$	$O4^{-2}$	$O4^{-1}$	$O4^{-2}$

Note that the first and third state are asymmetric in charge distribution, and hence possess a dipole momentum along the c-axis. The fourth state also has a dipole momentum but along the chain. For simplicity we shall neglect this state in our qualitative model since it does not contribute directly to IR activity of the 155-mode polarized along the c-direction.

In the $YBa_2Cu_3O_6$ system we have quite a different situation. The oxygens $O1$ are removed from the chains, and one part of their electrons fills the d-shells of $Cu1$ ions, while the remainder is transferred to the conducting sheets CuO_2. The total charge of our cluster is then reduced to -3. Consequently both the p-shells on $O4$ oxygens and d-shell on $Cu1$ copper ion in the cluster are completely filled and no low energy charge transfer fluctuation is possible. There exists only one formal charge state of the cluster: $O4^{-2}$, Cu^{1+}, O_4^{-2}.

The fluctuations between formal charge states in the $YBa_2Cu_3O_7$ cluster, can be described approximately by the following Hamiltonian,

$$H_{el}\begin{Bmatrix} e_2 & t & 0 \\ t & e_1 & t \\ 0 & t & e_2 \end{Bmatrix}. \qquad (8)$$

Here, the diagonal matrix elements e_1, e_2 correspond to the energies of the microscopic states, while the off-diagonal term t is the transition amplitude from one state to another. The Hamiltonian (8) can also be associated with a "single particle" Hamiltonian describing the motion of a hole among the $Cu1$ and two $O4$ ions. In this sense e_1 and e_2 are on-site energies of the hole on the $Cu1$ and $O4$ ions. The direct hopping between two $O4$ oxygens is neglected. Note that the microscopic state of the $YBa_2Cu_3O_6$ cluster is the situation when the hole is removed from the system. We shall frequently refer to Hamiltonian (1) as an "electronic" part of the total Hamiltonian, since the charge transfer fluctuations are nothing but electron motion within the cluster. The effects of including electron correlation effects within the cluster (e.g. Hubbard U and V_1) will be reported elsewhere. Here we only note that their major effects are to renormalize the parameters in Eq.(8): it is important to appreciate that the levels used are implicitly fully dressed many-body ones.

The matrix elements of H_{el} quite generally depend on the lattice deformation of the unit cell of $YBa_2Cu_3O_{7-\delta}$. We are particularly interested in the coupling of the charge transfer fluctuations to the 155-mode. The 155-mode is associated with almost rigid motion of the whole CuO_3 cluster between the CuO_2 sheets. This motion will primarily change the energies e_1, e_2, rather than the hopping amplitude t. The counterpart of the 155-mode is the Raman active mode corresponding to the symmetric oscillation of the $O4$ ions within the cluster. The frequency assigned to this Raman mode is 515 cm^{-1}. Both modes can be described approximately by the asymmetric and symmetric oscillations, respectively, of the $O4$ oxygens in the c-direction. Let Δ_1 and Δ_2 denote shifts of the $O4$ oxygen ions from their equilibrium positions. Keeping only terms linear in $\Delta_{1,2}$ in a Taylor expansion of e_1, e_2, we obtain the interaction Hamiltonian between the phonon and charge transfer fluctuations.

$$H_{el-ph} = -\lambda \begin{pmatrix} \Delta_1 & 0 & 0 \\ 0 & -\Delta_1 + \Delta_2 & 0 \\ 0 & 0 & -\Delta_2 \end{pmatrix}, \qquad (9)$$

where λ is the coupling constant. Other forms of electron-phonon couplings can also be included (e.g. through t) and lead to similar results. Note also that eq. (9) is oversimplified: there is in fact a (small) asymmetry to the coupling constants for IR and Raman modes.

We assume that the "phonon part" of the Hamiltonian is given by the familiar expression

$$H_{ph} = \frac{1}{2}K(\Delta_1^2 + \Delta_2^2) + \frac{1}{2}M(\dot{\Delta}_1^2 + \dot{\Delta}_2^2), \qquad (10)$$

where M and K are effective mass and elastic constant, respectively.

The Hamiltonians (9) and (10) can be rewritten in terms of coordinates corresponding to the asymmetric (IR) and symmetric (Raman) modes:

$$u, v = \frac{\Delta_1 \pm \Delta_2}{\sqrt{2}}. \qquad (11)$$

The model defined by the Eqs. (8-10) is quite general. It can alternatively be associated with the charge transfer fluctuations between the CuO_2 planes and CuO_3 cluster. In this case we assign the following formal charge states

$$
\begin{array}{ccc}
[CuO_2]^{-1} & [CuO_2]^{-2} & [CuO_2]^{-2} \\
| & | & | \\
[CuO_3]^{-4} & [CuO_3]^{-3} & [CuO_3]^{-4} \\
| & | & | \\
[CuO_2]^{-2} & [CuO_2]^{-2} & [CuO_2]^{-1} \ ,
\end{array}
$$

described again by Hamiltonian (1). The phonon modes Δ_1 and Δ_2 now correspond to the motion of the sheets CuO_2 with respect to the chain unit CuO_3, which is also part of displacements involved in the 155-mode. Conradson and Raistrick [10] have emphasized the importance of this charge transfer channel from an analysis of their EXAFS/XANES data. Presumably this charge transfer fluctuation also contributes to the IR activity of 155-mode. The most important charge transfer has yet to be unambiguously assigned but ab initio quantum chemistry is in progress [34] and finds a strong enhancement of the dipole derivative for the rigid c-axis motion of a CuO_4 cluster. This enhancement is a combination of the inherent oxygen polarization and charge transfer excitations within the cluster. Note that from a solid state model perspective oxygen polarizability may also be included via anharmonic electron-phonon coupling, in the spirit of shell models.[13]

Our model is a generalization of a two level system arising in many physics contexts. In fact a simrilar two level system has already been applied for the anomalous IR activity of the 240-mode in La_2CuO_4 [35] The scenario presented here can apply in a plane cluster through coupling to an appropriate phonon, and evidence for in-plane (e.g. Jahn-Teller, breathing, buckling) phonon modes has been reported [6].

The interaction Hamiltonian (9) will result in a renormalization of both IR and Raman phonon frequencies. It can also cause a static deformation of the cluster, which may be important for understanding of the structural transformations observed by Cava et al.[31] The renormalized frequency can be found within the usual RPA treatment of the interaction (9), Fig. 2a. In the case of the IR mode the renormalized frequency is given by

$$
\omega_{IR}^2 = \omega_0^2 - \frac{\lambda^2}{M_{eff}} \Pi_{MM}(\omega) \ , \tag{12}
$$

where ω_0 is the bare phonon frequency, $\sqrt{\frac{K}{M_{eff}}}$, while Π_{AB} is the electron polarization,

$$
\Pi_{AB} = i \int \frac{d\varepsilon}{2\pi} Tr(G(\omega + \varepsilon) A \ G(\varepsilon) \ B) \ . \tag{13}
$$

In the above expression $G(\omega)$ is the electron Green function equal to

$$
G(\omega) = [\omega - H_{el}]^{-1} \ . \tag{14}
$$

The pole of $G(\omega)$ with the lowest real part is shifted in the upper part of the complex ω plane, while the others poles are shifted into the lower part of the ω plane. The matrix M in expression (12) is the part of the interaction (9) corresponding to the IR mode, viz.

$$
M = \frac{1}{\sqrt{2}} \begin{pmatrix} 1 & 0 & 0 \\ 0 & 0 & 0 \\ 0 & 0 & -1 \end{pmatrix} \ . \tag{15}
$$

From expression (13) we can obtain the real part of the electron polarization and hence the change of frequency of the IR mode due to the electron-phonon interaction (9):

$$\frac{\delta(\omega^2)}{\omega^2} = \frac{\lambda^2}{M_{eff}\omega_0^2}\,\Pi_{MM}(0)\,. \qquad (16)$$

In $YBa_2Cu_3O_6$ there are no relevant charge transfer fluctuations, and consequently the frequency of the IR mode (and the frequency of any other mode) remains unchanged, i.e. ω_0. The above expression is therefore the relative difference between the frequencies of the 155-mode for $YBa_2Cu_3O_7$ and $YBa_2Cu_3O_6$ systems. It has been found experimentally that this difference is $\simeq 10\%$ (for $YBa_2Cu_3O_7$ $\omega_{IR} \simeq 155\ cm^{-1}$, while for $YBa_2Cu_3O_6$ $\omega_{IR} \simeq 168\ cm^{-1}$).[7] The right-hand side of Eq. (16) is proportional to a conventional definition of the dimensionless electron-phonon coupling constant,

$$\lambda = \frac{\lambda^2}{M_{eff}\omega_0^2 W}\,,$$

where W is the width of the excitation spectrum of the charge transfer fluctuations

$$2\sqrt{2t^2 + \left(\frac{\epsilon_2 - \epsilon_1}{2}\right)^2}\,.$$

In order to find the polarizability we need to determine the operator $\dot{P}$ of the dipole momentum of the system. This contains several terms with different origins,

$$\dot{P} = \sqrt{2}(Q\,u - p_o\,M)\,. \qquad (17)$$

The first term is the dipole momentum induced by the asymmetric motion of $O4$ ions. Here Q is the oxygen charge and u is the displacement of the IR mode defined in Eq. (11). The second electronic term depends on the microscopic state of the cluster. The quantity p_o is the dipole momentum of the first (third) microscopic state; it is of the order of the electron charge multiplied by the distance between $Cu1$ and $O4$ ions. M is a matrix defined by Eq. (15). In the case of the plane-chain-plane cluster, Q is the averaged charge of the CuO_2 planes per unit cell, while p_o is of the order of the electron charge multiplied by the distance between $Cu1$ and $Cu2$ ions.

The polarizability α of the system is given by the correlation function of the dipole momentums. The phonon part of $\dot{P}$ leads to the familiar lattice dynamics term,

$$\alpha_{ph}(\omega) = 2\,\frac{Q^2}{M_{eff}}\,\frac{1}{\omega_{IR}^2 - \omega^2}\,. \qquad (18)$$

The electron part of the polarizability is proportional to the polarization Π_{MM}.

$$\alpha_{el}(\omega) = 2p_o^2\,\Pi_{MM}(\omega)\,. \qquad (19)$$

This is the zeroth order term in the electron-phonon interaction. The RPA treatment of the interaction (9) results in an additional term with a pole at the phonon frequency ω_{IR}.

$$\delta\alpha_{el}(\omega) = 2\,\frac{(p_o\lambda\Pi_{MM})^2}{M_{eff}}\,\frac{1}{\omega_{IR}^2 - \omega^2}\,. \qquad (20)$$

In $YBa_2Cu_3O_6$ this additional term is absent because the charge transfer fluctuations are suppressed. The combination of the Eqs. (18) and (20) gives the polarizability with an effective oscillator strength equal to

$$f = 2\,\frac{Q^2}{M_{eff}\omega_0^2}\,(1 + (\frac{p_0\,\lambda\,\Pi_{MM}(0)}{Q})^2) \qquad (21)$$

for the 155-mode. The difference δf between the oscillator strengths of this phonon mode in $YBa_2Cu_3O_7$ and $YBa_2Cu_3O_6$ systems is therefore given by

$$\frac{\delta f}{f} = (\frac{p_0\,\lambda\,\Pi_{MM}(0)}{Q})^2 . \qquad (22)$$

According to the measurements of Genzel et al. [7] the quantity (22) is equal to 15.

Equations (16) and (22) can be used for independent estimates of the coupling constant λ for $YBa_2Cu_3O_{7-\delta}$. If we assume that the polarization $\Pi_{MM}(\omega = 0)$ is given by the inverse of the typical energy of the charge transfer fluctuations[16], i.e. of the order of $(0.1\ eV)^{-1}$, then, according to the Eq. (16) the coupling constant is

$$\lambda \simeq 0.12\,\sqrt{\frac{M_{eff}}{M_O}}\,\frac{eV}{\AA} ,$$

while from Eq. (22) it follows that

$$\lambda \simeq 0.19\frac{eV}{\AA} .$$

Here, M_O stands for the oxygen mass. In order to improve agreement between these two estimates it is necessary to assume that the effective mass M_{eff} of the 155-mode is of the order of four oxygen masses: this effective mass requirement increases if the energy of the charge transfer fluctuations increases (i.e. Π^{-1}_{MM}) 0.1 eV). The estimated values of λ are relatively small in comparison to coupling constants in some other materials, e.g. polyacetylene. Interestingly, other estimates of λ based on the superconducting transition temperatures lead to similar values.[36]

The static deformation of the corresponding symmetric (Raman) mode is given by the averaged value of its interaction with CT fluctuations,

$$v_0 = \frac{\lambda}{\sqrt{2}K}\,(\begin{pmatrix} 1 & 0 & 0 \\ 0 & -2 & 0 \\ 0 & 0 & 1 \end{pmatrix})_o . \qquad (23)$$

For $YBa_2Cu_3O_7$, v_0 exists for any finite value of the coupling constant λ, and is equal to

$$v_0 = -\frac{\lambda}{2\sqrt{2}M_{eff}\omega_0^2}\,(1 + \frac{3(e_2 - e_1)}{2\sqrt{2t^2 + (\frac{e_2 - e_1}{2})^2}}) . \qquad (24)$$

However this deformation is equal to zero in $YBa_2Cu_3O_6$. The expression (24) corresponds therefore to the difference of the $Cu1$-$O4$ distances in $YBa_2Cu_3O_7$ and $YBa_2Cu_3O_6$ systems, which is found experimentally to be equal to 0.04 Å, or $\approx 2\%$. The static deformation of the Raman mode will also renormalize the on-site energies, so that the energies e_1 and e_2 are shifted by $2\lambda v_0/\sqrt{2}$ and for $-\lambda v_0/\sqrt{2}$ respectively. For self consistency we must take into account these corrections in all previous expressions. Alternatively, for the plane-chain-plane cluster the static deformation (24) is measured to be equal 0.13 Å, or $\approx 3\%$.

A static deformation of the asymmetric (IR) mode is possible only for sufficiently large coupling constants λ. The critical value of λ can be estimated from the expression (3) by

requiring that the renormalized frequency ω_{IR} is equal to zero. Since the change of the frequency in the IR mode is proportional to the dimensionless coupling constant, we find that the necessary condition for this transition is $\tilde{\lambda} \geq \frac{\omega_0^2 r}{t^2} \sim 1$. Note that such a static deformation of the IR mode will induce a permanent dipole momentum in the unit cell, and it is therefore to be associated with an (*anti-*)ferroelectric transition.[37] In this region of parameter space, the dynamics of the IR phonon mode is essentially nonlinear. The corresponding equation of motion of this mode can be found in an adiabatic approximation valid for $t^2 \gg \lambda \dot{u} \approx \lambda u \omega_{IR}$. For small phonon displacements, we obtain an equation with a dominant cubic nonlinearity:

$$M\ddot{u} = -K\, u + K\, \tilde{\lambda}\, \frac{2t^2}{\omega_0^2 \tilde{C} T}\, u(1 - (\frac{u}{u_o})^2) \,, \tag{23}$$

where the coefficient of the nonlinear term is

$$u_o^{-2} = \frac{\lambda^2}{W^2 \omega_0^2 \tilde{C} T}(2t^2 + W(e_1 - e_2)) \,.$$

Clearly, the three level model defined by Eqs. (8-10) can be used only for some special composition of the $YBa_2Cu_3O_{7-\delta}$. Namely, the number of the holes within the cluster can be changed only discontinuously, in our case from the one hole to the case with no holes. As we have already discussed, these two cases correspond to the compositions with $\delta = 0$ and $\delta = 1$ respectively. However, in a case with an intermediate composition $0 < \delta < 1$, the crystal of $YBa_2Cu_3O_{7-\delta}$ consists of the clusters with one hole and the clusters without holes. The most simple approach to such situation is the *virtual crystal approximation*. (Extension to a coherent potential approximation is also straightforward.) According to this approximation the overall electron Green function is given by the linear interpolation of the Green functions of the two limiting known cases,

$$G(1 \geq \delta \geq 0) = x\, G(\delta = 1) + (1 - x)\, G(\delta = 0) \,.$$

Here parameter x is the fraction of the clusters with no holes. According to the measurements of Tranquada et al.,[32] this parameter is nothing but the number of the Cu^{+1} ions per unit cell, and it is equal approximately to δ for $\delta < 0.6$, while for $\delta > 0.6$ it is $\approx 2\delta - 1$. By using the formula (13) for the electron polarization, we find that Π_{MM} is proportional to $(1 - x)$,

$$\Pi_{MM}(1 \geq \delta \geq 0) = (1 - x)\, \Pi_{MM}(\delta = 0) \,.$$

The composition dependence of the frequency of the IR-mode can be obtained from Eq. (12). It is given by a linear interpolation of the frequencies for $\delta = 0$ and $\delta = 1$,

$$\omega_{IR}(1 \geq \delta \geq 0) = x\, \omega_{IR}(\delta = 1) + (1 - x)\, \omega_{IR}(\delta = 0) \,.$$

A nonlinear behavior in δ of the frequency ω_{IR} is expected only for δ close to 0.6, when an orthorhombic-tetragonal transition occurs. The electron contribution to the oscillatory strength of the IR-mode is quadratic in the electron polarization Π_{MM}, and consequently it will show a more dramatic δ-behavior. It decreases linearly for $\delta \geq 0$, and eventually for $\delta \leq 1$ it disappears as $(\delta - 1)^2$. The virtual crystal approximation also predicts the linear x-behavior of the static deformation of the Raman mode. Associated with such a static deformation there is also a self-consistent change in the hole density in the planes/chains. This is presumably reflected in the rapid change in T_c at $\delta \sim 0.5$.

Finally, we note that more detailed microscopic modeling of phonon-CT coupling requires studies of clusters explicitly including, e.g., Hubbard U and V and electron-phonon interactions. Such studies are in progress.

2(iii) Pairing-Bag excitations

Here we focus on one aspect of strong coupling (small coherence length) superconductors, namely the possibility of polaron or bag-like deformation of the condensate, which may have distinct experimental consequences -- e.g. for observations of the tunneling density of states and assignment of a SC "gap."

In the pairing theory of superconductivity, the ground-state energy gap Δ is uniform in space for a translationally invariant system.[38] When a single quasiparticle is added to the system, the gap is assumed to remain uniform so that the excitation is in a plane-wave state k. As in Koopmans's theorem for the Hartree-Fock approximation to extended sytems, Δ is unaltered by the presence of the excitation as the volume of the system tends to infinity.

For nonzero temperature, the gap decreases because of the finite density of quasiparticles, with Δ vanishing at the transition temperature T_c, where the quasiparticle density is of order $(\xi/a)^2$ per coherence volume ξ^3, with a the mean electron spacing and ξ the zero-temperature coherence length. Since $\xi/a \approx 10^3$ for conventional superconductors, the depression of the gap by the addition of *one* quasiparticle in a coherence volume is extremely small.

However, for the new layered high-temperature superconductors the corresponding ξ/a is of order 1-10. Therefore, when a quasiparticle is excited in a coherence volume the gap is locally substantially reduced even at zero temperature. This reduction forms a baglike potential which, if sufficiently strong, self-consistently traps the quasiparticle, as in a self-trapped polaron. Here the pairing field plays the role of the phonon field of the polaron.

We study the structure of such localization pairing-bag solutions to the Bogoliubov-de Gennes equations on a two-dimensional square lattice in the context of the "negative-U" Hubbard model.[39] As in the case of spin bags.[40] for a half-filled band we find self-consistent solutions for Δ which have "cigar" or "star" shapes depending on the symmetry of the orbital in which the quasiparticle is initially placed, as well as the initial spatial form of Δ. While these solutions break translational symmetry, this can be restored by forming linear combinations of such localized configurations suitably phased to create a momentum eigenstate.

We consider the negative-U Hubbard model on a 2D square lattice to model the CuO_2 planes in the oxide superconductors. The Hamiltonian is

$$H = -\sum_{nms} t_{nm} c^\dagger_{ms} c_{ns} - \sum_{nm} V_{nm} c^\dagger_{m\uparrow} c^\dagger_{n\downarrow} c_{n\downarrow} c_{m\uparrow} \,. \tag{26}$$

In the mean-field pairing approximation for the superconducting phase one has

$$H = -\sum_{nms} t_{nm} c^\dagger_{ms} c_{ns} - \sum_{nm} [\Delta^*_{nm} c_{n\downarrow} c_{m\uparrow} + H.c. - |\Delta_{nm}|^2 / V_{nm}] \,, \tag{27}$$

with the self-consistency condition

$$\Delta^*_{nm} \equiv V_{nm} \langle 0 | c^\dagger_{m\uparrow} c^\dagger_{n\downarrow} | 0 \rangle \,, \tag{28}$$

where V_{nm} is positive for an attractive potential and $|\phi\rangle$ is a quasiparticle occupation number state. H can be diagonalized by making the Bogoliubov-Valatin transformation:

$$c_{ns}^{\dagger} = \sum_{i} [u_{ni}^{*} \gamma_{is}^{\dagger} + \nu_{nis} \gamma_{i,-s}] . \tag{29}$$

Here $\gamma_{is}^{\dagger}$ are the quasiparticle creation operators.

$$[H, \gamma_{is}^{\dagger}] = E_{is} \gamma_{is}^{\dagger}, \quad [H, \gamma_{is}] = -E_{is} \gamma_{is}, \quad E_{is} \geq 0 . \tag{30}$$

Without loss of generality we have chosen phases so that u_{nis} is spin independent. The u and ν amplitudes can be determined by our taking matrix elements of the equation of motion of the bare operators c between an initial state $|\phi\rangle$ and the state having one more quasiparticle in orbital i. As usual, we work within the grand canonical ensemble. Using $\nu_{nis} = -\nu_{ni}$ one finds

$$E_i u_{ni} = \sum_{m} [-t_{nm} u_{mi} + \Delta_{nm} \nu_{mi}] , \tag{31}$$

$$E_i \nu_{ni} = \sum_{m} [t_{nm} \nu_{mi} + \Delta_{nm}^{*} u_{mi}] , \tag{32}$$

and the self-consistency condition becomes

$$\Delta_{nm} = V_{nm} \sum_{i} [u_{ni} \nu_{mi}^{*} (1 - N_{i\downarrow}) - u_{mi} \nu_{ni}^{*} N_{i\uparrow}] , \tag{33}$$

where N_{is} is the quasiparticle occupation number. Evaluating the expectation value of H in the state $|\phi\rangle$, we find the total energy given by

$$E_{\phi} = -\sum_{i} E_i \left(1 - \sum_{s} N_{is}\right) + \sum_{nm} \frac{|\Delta_{nm}|^2}{V_{nm}} . \tag{34}$$

For an $N \times N$ lattice, we note that there are $2N^2$ amplitudes u_n and ν_n. While this leads to $2N^2$ eigenvalues E_i, only the positive values of E_i correspond to the energy required to create a quasiparticle, whether it be a quasielectron above the Fermi surface, or a quasihole below; all physical excitation energies are necessarily positive. The negative eigenvalues correspond to the energy released when a quasiparticle (either electronlike or holelike) is destroyed. Therefore, we are only interested in the positive-energy solutions, and sum only over $E_i > 0$ in (34).

We have solved the equations numerically on periodic $N \times N$ square lattices with $N = 4$ to 16. Extremal solutions to the coupled equations (31) and (32) were sought by iteration in $\{u_{ni}, \nu_{ni}\}$ until self-consistency (33) was obtained [39] for a given quasiparticle occupation, with various initial Δ_{nm} profiles as "seeds." The eigenvalue distribution E_i and symmetries of the associated eigenvectors $\{u_{ni}, \nu_{ni}\}$ were studied. To illustrate bag states we show here results for a *local* "negative U", $V_{nm} = V_0 \delta_{nm}$, and pure *near-neighbor*, isotropic hopping of strength t. In Fig. 4(a) we show the result of placing one additional quasiparticle in an orbital near the flat region of the square Fermi surface. Localization occurs, mirroring the symmetry of this orbital and producing a cigar shape. If orbitals near corners of the square Fermi surface are occupied, the localized state assumes their symmetry -- the crossed cigar or star shown in Fig. 4(b). The local deformations of δ_{nm} are accompanied (see figure captions) by an eigenlevel being drawn into the uniform gap

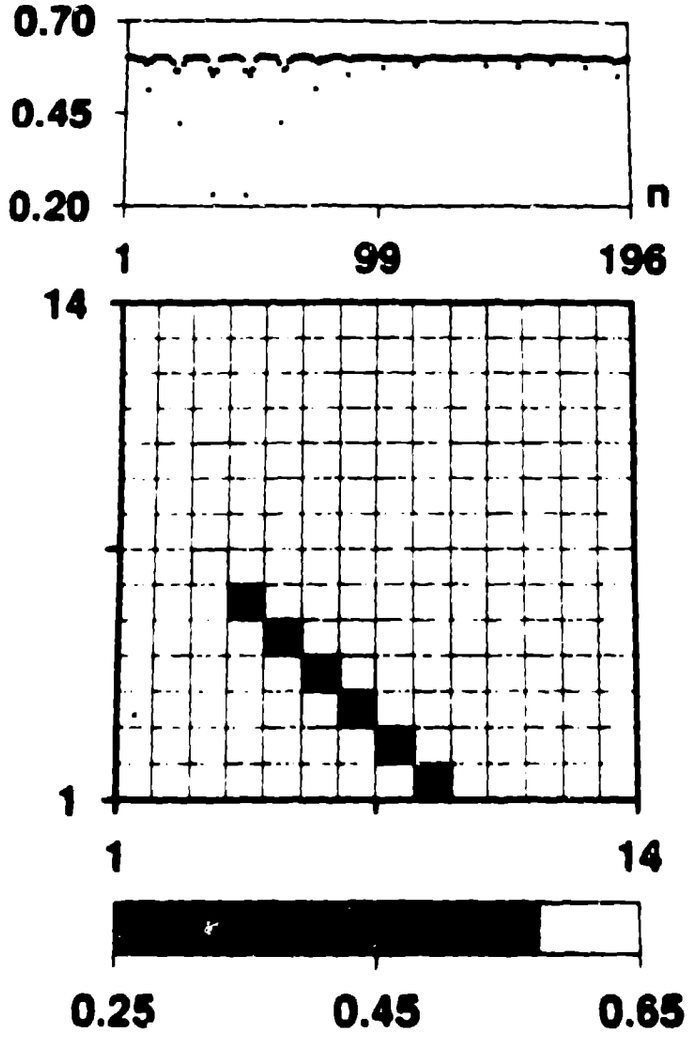

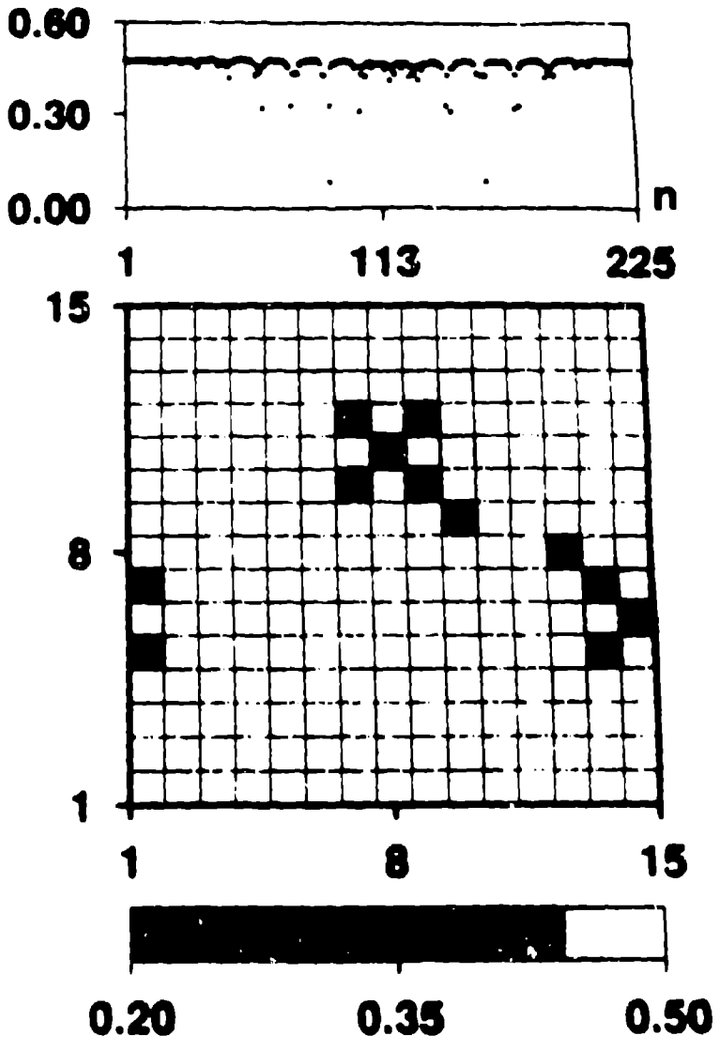

Figure 4(a). One quasiparticle has nucleated a cigar-shaped bag on a 14×14 lattice with periodic boundary conditions and $V_0 = 2.5t$. The top part of the figure shows Δ vs the site index n in a linear array (row by row). The lower part shows Δ on the square lattice as a gray-scale plot. The bag was seeded at the sites where it nucleated. The energy level of the quasiparticle is pulled into the gap. Its value is $0.430t$ and the band of higher levels starts at $0.566t$.

Figure 4(b). Two quasiparticle occupying the two lowest energy levels have formed two star-shaped bags on a 15×15 lattice for $V_0 = 2.25t$. The energy levels are again pulled into the gap and are almost degenerate, with values $0.363t$ and $0.366t$. The band of higher energy levels starts at $0.464t$. Note that the orientation of the stars was seeded to be slightly off diagonal in this case.

present in the absence of added quasiparticles: the greater the localization, the deeper the gap state. The remaining continuum states suffer energy-level shifts which are limited to near-gap states as the bag becomes more delocalized. The binding energy E_b of a bag also increases with V_0/t, where the binding energy is defined relative to an added quasiparticle with uniform Δ. For example, on an 10×10 lattice and for star bags in the same initial Fermi-surface orbital, we find $(V_0/t, \Delta/t, E_b/t)$ with values (2.5,0.615,0.088) and (3.0,0.854,0.147). In general the star bags seems to have a few percent greater binding energy than the corresponding cigar bags.

Inclusion of quantum fluctuations around the bag states described above is in progress. As in the strong-coupling polaron, the true quantum mechanical states must be constructed out of the present broken-symmetry states by a phased, translationally invariant sum, to yield a *band* of bag states. Note that the hole and order-parameter field must move together at a large velocity ($\approx v_f$). This motion is expected to deform the bag, determine limiting velocities, and even prevent the condensate from following the hole in some cases. The influence of a chemical potential will also be reported elsewhere -- the large density of states at half-filling is most favorable for superconductivity, but varying electron density changes the Fermi-surface structure and therefore bag shapes.

The physical consequences of such pairing-bag states are under investigation, including electromagnetic absorption, quasiparticle and Josephson tunneling, thermodynamics, fluctuation effects, quasiparticle recombination, etc. We have also developed a time-dependent extension of the present theory, which will allow study of dynamics of bag-formation and their interactions, localized bag oscillations, and decay channels -- for instance of quasiparticle excited states to the uniform ground state by phonon and microwave emission.

2(iv) Halogen-bridged transition metal linear chain crystals

These materials have been of interest to chemists for several decades [41]. However, they have only recently begun to receive systematic attention and detailed consideration in the physics community [42]. While they are important in their own right, it should be stressed that they represent a controlled class of materials in which to probe many of the issues raised by the new oxide superconductors -- in terms of theoretical techniques, collective ground state mechanisms, doping- and photo-induced defects, and experimental characterization. Indeed typical members of the class are direct 1-dimensional analogues [43] of $BaPb_{1-x}Bi_xO_3$ and lead to our current efforts to *dope* the 1-dimensional materials near transitions between (e.g. charge- and spin-density-wave) ground states. More specifically, we emphasize here:

(a) The increasing appreciation of strong, competing electron-electron and electron-phonon interactions in low-dimensional materials and the consequent need to expand many-body techniques. The MX materials offer a rapidly expanding, single-crystal class of quasi-1-D systems which can be "tuned" (by chemistry, pressure, doping, etc.) between various ground state extremes: from strong charge-disproportionation and large lattice distortion (e.g., PtCl - 20% distortion) to weak charge-density-wave and small lattice distortion (e.g., PtI - 5% distortion), to magnetic and undistorted (e.g., NiBr);

(b) The opportunity to probe doping- and light-induced local defect states (polarons, bipolarons, kinks, excitons) and their interactions in controlled environments and the same large range of ground states;

(c) The similarities between models and theoretical issues in these materials and the recently discovered high-temperature superconductors. The MX materials are also closely connected conceptually with mixed-stack charge-transfer salts.

The MX class, then, is important in its own right, but also as a testing ground for concepts and electronic structure techniques in strongly interacting (both electron-electron

and electron-phonon), low-D electronic materials. A joint theoretical effort is underway to give a unified understanding of these materials from the different points of view of band-structure calculations (valid in the delocalized limit), ab initio quantum chemistry calculations (valid in the high localize limit), and many-body Hamiltonians.

From a band structure point of view, the MX class is essentially a hybridized 2-band (M and X majority) system in which the antibonding band is half-filled at stochiometry with several nonbonding levels between the bands. In the ionic limit for, e.g., M=Pt, X=Br one has a filled Pt d_{z^2} orbital and a half-filled Br p_z orbital, i.e. 6 electrons per MX unit. The structure of a single chain is shown schematically in Fig. 5. Coupling between adjacent chains is small and the ligands appear to be of secondary importance for the electronic structure along the chain. When filled non-bonding levels lying between the bonding and antibonding bands are included, as well as the extended Hubbard and strong (nonlinear) electron-phonon coupling terms, we see that we have a 1-D version of our previous description for CuO_2 planes (and chains) in the superconducting oxides. However, here we have advantages of tunability of model parameters and of single crystal materials.

For instance, focusing on a single orbital per site and including only nearest neighbor interactions, we have investigated [44] the following two-band model for an isolated MX chain:

$$\begin{aligned} H = \sum_{l,\sigma} \{ (-t_0 + \alpha \Delta_l)(c^\dagger_{l,\sigma} c_{l+1,\sigma} + c^\dagger_{l+1,\sigma} c_{l,\sigma}) + [(-1)^l 2e_o - \beta_l(\Delta_l + \Delta_{l-1})] c^\dagger_{l,\sigma} c_{l,\sigma} \} \\ + \sum_l U_l n_{l\uparrow} n_{l\downarrow} + V \sum_l n_l n_{l+1} + V_{MM} \sum_{l\ even} n_l n_{l+2} \\ + \frac{K}{2} \sum_l \Delta_l^2 + \frac{K_{MM}}{2} \sum_l (\Delta_{2l} + \Delta_{2l+1})^2 + \frac{1}{2} \sum_l \frac{\hat{p}_l^2}{M_l} , \end{aligned} \tag{35}$$

with $\beta_l = [\beta_X, \beta_M]$, $U_l = [U_X, U_M]$, relative coordinates $\Delta_l = \hat{u}_{l+1} - \hat{u}_l$, momenta $\hat{p}_l$, and displacements from uniform lattice spacing $\hat{u}_l$. This is, of course, a discrete tight-binding extended Peierls-Hubbard model with $2e_o = e_M - e_X$ ($e_{M,X}$ being on-site affinities), intra (β)- and inter (α, breathing)-site electron-phonon coupling, and an effective M-X spring (K). In addition a metal-metal spring (K_{MM} tends to preserve a uniform M-M distance, representing the "cage" effect of the 3-dimensional network.

It is not our intention to review the M-X materials here. We merely note that the full spectrum of analytic and numerical techniques used for oxide systems is also being employed [44]. This investigation has revealed a rich set of collective ground states as parameters are varied: charge-density-wave, bond-order-wave, spin-density-wave, spin-Peierls, etc. Correspondingly, defects (kinks, polarons, bipolarons, excitons) have been studied with respect to these various ground states. While expectations of superconductivity may be optimistic, interesting behavior is indicated near the transitions between ground states, where fluctuations of competing phases are soft. For this reason there is a systematic experimental program using chemistry, pressure and doping to "tune" into these regimes.

Finally, we note that simple dimerized patterns are not the only ground states of Hamiltonian (35). We have found, for example, that strong on-site electron-phonon coupling, in the presence of Coulomb interactions, drives a hierarchy of long-period (superlattice) ground state states [45]. This will also occur in higher-dimensional analogs and it is intriguing to speculate that Hamiltonians such as (35) may contain not only the secret of superconductivity but also intrinsic microscopic mechanisms for the "twinning" and superlattice structures which seem to be so characteristic of the new oxide superconductors.

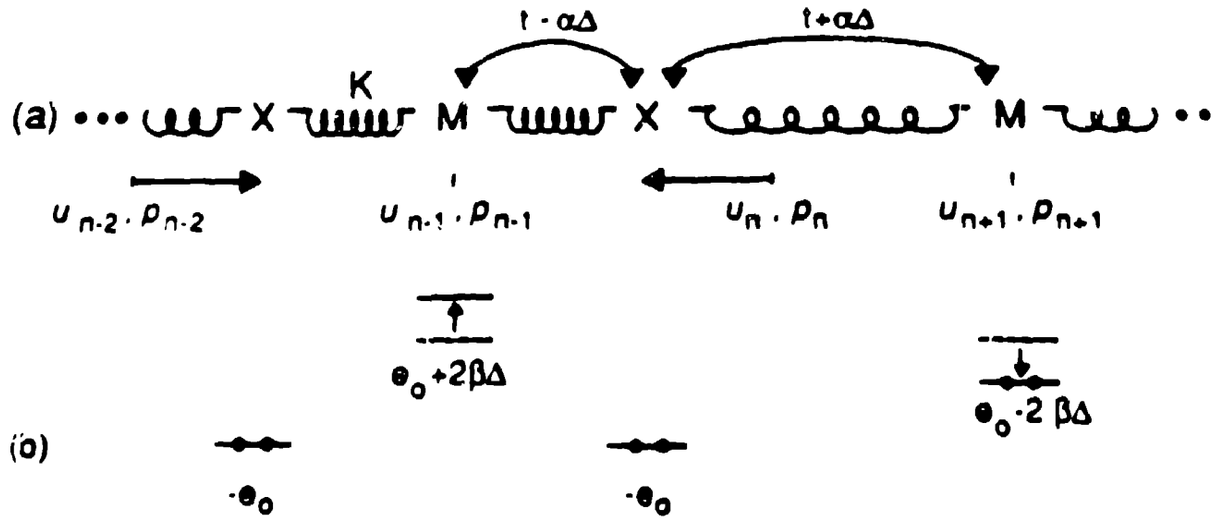

Figure 5. (a) Schematic of the MX chain showing the model parameters and a CDW distortion; (b) the corresponding $t_0 = \alpha = 0$ energy levels.

3. Discussion

A microscopic theory of HTC in oxide superconductors is still not available. Given the 10 year histories of heavy fermion and organic mixed stack superconductors (see these proceedings) this is not so surprising. In this article we have indicated several strategic lines of thinking: (i) Transition metal oxides are distinguished generally by strong competitions for broken symmetry ground states of many varieties. Superconductivity is an "eye-of-the-needle" problem of operating near transition between other broken symmetry states, where soft fluctuations can be used for pairing, without freezing into those alter-

native ground states; (ii) We have argued that, although charge and spin fluctuations will inevitably coexist in these small coherence length materials, charge fluctuations may play the dominant role. In $Ba_xK_{1-x}BiO_3$ this is natural, since a disproportional (charge-density-wave) reference state is close to superconductivity. In the copper-based HTC materials, the stoichiometric materials is dominated by an antiferromagnetic spin instability (as in organic superconductors). We have argued that the role of hole doping is to drive proximity to alternative incipient charge-density-wave instabilities, possibly including a strong short range antiferromagnetic spin component; (iii) Very high superconducting transition temperatures are problematical within conventional BCS/Eliashberg mechanisms using phonons, spin *or* charge as the pairing boson. We have however argued that a synergistic *coupling* of phonons with charge (or possibly spin) is natural in these perovskite-like materials. Furthermore *anharmonic* (large-amplitude) lattice distortions are also natural here. We have argued that *coupling* of phonons to C-T channels can drive the soft phonon distortions, which can then augment underlying charge/spin pairing mechanisms. This can happen purely in the plane (in $La_{1-x}Sr_xCuO_4$). However, further enhancement is possible in 1-2-3 and other truly layered materials, using the dynamic polarizability of the material surrounding the planes. This polarizability can induce pairing in the plane using the polarization fluctuations. *Alternatively*, the C-T excitations microscopically comprising the polarizability (section 2(i)) can couple to, and act as a "pump" for, soft phonons in the plane [1.22] (e.g. the buckling mode [33]) driving them into anharmonic regimes and leading to the scenario suggested above. Such a scenario relies on a combination of specific structural and chemical features in these materials, and should not be confused with simple charge fluctuation pairing.

Thus, we believe that serious attention should now be devoted to superconductivity within *strong coupling* BCS theory, but with coexisting and coupled C-T (excitonic) and phonon channels, possibly with relatively strong effects of electron-electron (Coulomb) interactions (e.g., antiferromagnetic spin fluctuations). Such theories are not constrained by the T_c limitations of pure phonon coupling but need some developments beyond familiar Eliashberg theory - - including vertex corrections, for instance.

Some preliminary steps including multiple channels additively in the Eliashberg function ($\alpha^2(\omega)F(\omega)$) have been taken [46]. A coupling of channels should be investigated, however. In addition, it seems likely that strongly *anharmonic* phonons are necessary. Again, preliminary steps to generalize Eliashberg theory have been taken [47], but much remains to be done - - it may be necessary to go beyond Fröhlich-level Hamiltonians to include the influence of the superconductivity on phonons (indicated by certain experiments [27]) self-consistently. Inclusion of double-well anharmonicity is an interesting first step, especially if we recall that descriptions of structural phase transitions in perovskites have traditionally used "shell" models, integrating out the electronic degrees of freedom (e.g. the oxygen polarizability) to leave effective anharmonic phonons. These real phonons can be used for pairing electrons (holes) as in conventional Eliashberg theory and will result in a temperature-dependent Eliashberg function with possibly distinctive consequences for isotropic shifts, effective values for $2\Delta(o)/k_BT_c$, etc.

Acknowledgments

I am grateful to all of my collaborators on the work reported here: I. Batistic, T. Gammel, P. Lomdahl, R. Martin, R. Schrieffer, Z. Tesanovic and S. Trugman.

References

1. A. R. Bishop, R. L. Martin, K. A. Mueller, Z. Tesanovic, Z. Physik B 76, 17 (1989); Solid State Comm. 68, 837 (1988).

2. Z. Schlesinger et al, preprint.

3. K. Kamoras et al, preprint.

4. K. Tanaka et al, Physica C 153-5, 1752 (1988).

5. Z. Tesanovic, private communication.

6. e.g., B. Renker et al, Z. Physik B67, 15 (1987); R. E. Cohen et al, Phys. Rev. Lett. 62, 831 (1989); M. Francois et al, Solid State Comm. 66, 1117 (1988).

7. L. Genzel et al, Phys. Rev. B (in press).

8. L. Bulaievskii et al, preprint.

9. C.-K. Loong et al, Phys. Rev. Lett. 62, 2628 (1989).

10. S. Conradson and I. Raistrick, Science 243, 1340 (1989); S. Conradson, I. Raistrick and A. R. Bishop, preprint (1989).

11. R. Zamboni, G. Ruani, A. J. Pal and C. Taliani, Sol. State Comm. 70, 813 (1989).

12. A. J. Arko et al, Phys. Rev. B (in press).

13. A. Büssmann-Holder, A. Simon, H. Büttner, Phys. Rev. B (in press).

14. J. E. Hirsch, preprint (1989).

15. A. Zawadowski, Sol. State Comm. 70, 439 (1989).

16. L. F. Mattheis, Phys. Rev. Lett. 58, 1028 (1987).

17. Holes in NB O_x orbitals have been suggested by, e.g., Y. Guo et al, Science 239, 896 (1988).

18. A. Shirane et al, Phys. Rev. Lett. 59, 1613 (1987).

19. J. M. Tranquada et al, Phys. Rev. Lett. 60, 156 (1988).

20. C. A. Balseiro et al, Phys. Rev. Lett. 62, 2624 (1989).

21. J. E. Hirsch et al, Phys. Rev. Lett. 60, 1668 (1988).

22. Z. Tesanovic, A. R. Bishop, R. L. Martin, C. Harris, in "Towards the Theoretical Understanding of High Temperature Superconductors," eds. S. Lundquist et al (World Scientific, Singapore 1988).

23. C. M. Varma, S. Schmitt-Rink, E. Abrahams, Solid State Comm. 62, 681 (1987); P. B. Littlewood et al, Phys. Rev. B 39, 12371 (1989).

24. e.g., D. Scalapino et al, Phys. Rev. B 34, 8190 (1986).

25. D. Baeriswyl and A. R. Bishop, Physica Scripta T19, 239 (1987).

26. C. M. Varma in "Proceedings of the Schloss Mautendorf Meeting on HTS," ed. H. W. Weber (Plenum, NY, 1988).

27. J. B. Torrance, Phys. Rev. Lett. 61, 1127 (1988).

28. J. B. Torrance et al, unpublished.

29. The cluster calculations were performed by R. L. Martin with the MESA codes designed by P. Saxe et al (Los Alamos National Laboratory).

30. I. Batistic, A. R. Bishop, R. L. Martin, Z. Tesanovic, Phys. Rev. B (in press).

31. R. J. Cava et al, Physics C156, 523 (1988).

32. J. M. Tranquada et al, Phys. Rev. B 38, 8893 (1988).

33. H. Monien and A. Zawadowski, preprint.

34. J. Hay and R. L. Martin, unpublished.

35. M. J. Rice and Y. R. Wang, Phys. Rev. B 36, 8794 (1987).

36. P. C. Pattnaik and D. M. Newns, Physica C157, 13 (1989).

37. Large c-direction dielectric constants have been reported by L. R. Testardi et al (Nature, in press) in $YBa_2Cu_3O_{7-\delta}$; but also in the a-b plane for La_2CuO_4 by D. Reagor et al (preprint). It is tempting to believe that a ferroelectric distortion, typical of polarizable perovskites, is nearby. However, note that for materials with mirror plane symmetry, *antiferroelectric* fluctuations should be sought. (See section 2(ii)).

38. J. Bardeen, C. N. Cooper, J. R. Schrieffer, Phys. Rev. 108, 1175 (1957)

39. A. R. Bishop, P. S. Lomdahl, J. R. Schrieffer, S. A. Trugman, Phys. Rev. Lett. 61, 2709 (1988); D. Coffey et al, preprint (1989).

40. J. R. Schrieffer, X.-G. Wen, S.-C. Zhang, Phys. Rev. Lett. 60, 944 (1988); Phys. Rev. B (in press).

41. e.g., P. Day, in "Low Dimensional Cooperative Phenomena," ed. H. J. Keller (Plenum, NY, 1974).

42. e.g., K. Nasu, J. Phys. Soc. Jpn. 52, 3865 (1983).

43. D. Baeriswyl and A. R. Bishop, J. Phys. C21, 339 (1988).

44. A. R. Bishop et al, Synthetic Metals **29**, F151 (1989); J. T. Gammel et al, Synthetic Metals 29, F161 (1989); and Los Alamos preprints.

45. I. Batistic et al, in preparation.

46. F. Marsiglio, M. Schossmann and J. P. Carbotte, Phys. Rev. B 37, 4965 (1987); J. M. Coombes and J. P. Carbotte, Phys. Rev. B 38, 8697 (1988).

47. N. M. Plakida, V. L. Aksenov, S. L. Drechsler, Europhys. Lett. 4, 1309 (1987); J. R. Hardy and J. W. Flocken, Phys. Rev. Lett. 60, 2191 (1988), and preprint (1989).